Supplementary Information 2 for

Chemical properties of the Southeast Asian haze from Indonesian peatland fires

Yusuke Fujii[1] and Susumu Tohno[2]

Global Environmental Research, Vol. 27, No. 1, pp. 37–48, 2023.

[1] Division of Sustainable System Sciences
Graduate School of Sustainable System Sciences
Osaka Metropolitan University
Naka-ku, Sakai, Osaka 599-8531, Japan

[2] Professor Emeritus, Kyoto University
Sakyo-ku, Kyoto 606-8501, Japan

Corresponding authors:
Yusuke Fujii (fujii.yusuke@omu.ac.jp), Susumu Tohno (tohno@energy.kyoto-u.ac.jp)

This supplementary information contains 12 tables, eight figures and additional documents relevant to the main article's Sections 4 and 6.

Supplementary Document Related to Items in Sections 4 and 6

4. Aerosol Mass Spectra Analysis for Chemical Characterization

S4.1 Chemical compositions

Laboratory-generated fresh aerosols from Indonesian peat combustion (hereafter, Lab-PM) had low f_{44} (m/z 44 ion fraction, indicative of degree of oxidation) and f_{60} values, but this depended on the sampling site (location) of the peat[66, 81]. In the case of the 2015 haze particles, the ubiquity and dominance of oxygenated species in organics, in line with the most intense ion signals at m/z 44 (mostly CO_2^+, f_{44} =0.105 in total OA mass) and m/z 43 ($C_3H_7^+$, $C_2H_3O^+$, typically pronounced for hydrocarbon-like organic materials, f_{43} =0.075 on average)[74].

The polarity-segregated water-soluble organic matter (WSOM) of Lab-PM filter samples obtained according to the 1-octanol−water partitioning method (Kuwata & Lee, 2017) was analyzed in combination with UV−visible and fluorescence spectrophotometers[86]. Three classes of WSOM[86] were obtained by applying several deconvolution methods to the measured OA spectra as shown in Table S3. The existence of HULIS with different polarities was also suggested[86].

The four source factors of OA in NR-PM_1 (haze particles) were identified and quantified, using ToF-ACSM with deconvolution of the OA mass in combination with an offline chemical analysis[73]. Three of them were primary organic aerosol (POA) factors and the remaining OA was a surrogate of both SOA and oxidized POA (OPOA), as shown in Fig. S7. Separation of OPOA and SOA mass spectra in oxygenated OA (OOA) could not be performed. These findings indicate POA oxidation and SOA formation to be important chemical processes during atmospheric transport of IPF aerosols.

The dependence of chemical compositions of Lab-PM on heating temperature was investigated, using ToF-ACSM and nuclear magnetic resonance (NMR) for filter samples[69]. In mass spectra of OA, the f_{44} were small, while the f_{43} were prominent and the aerosol particles emitted at higher temperatures had more unsaturated bonds and ring structures than those emitted at lower temperatures[69].

S4.2 Secondary aerosol formation (Aging)

SOA formation results from atmospheric oxidation of IPF-derived gaseous precursors and aqueous phase reactions with partitioning of water-soluble organic gases to atmospheric liquid water (aqSOA) (McNeill, 2015). To date, laboratory experiments using combustion and reaction chambers have been conducted to separate the contribution of POA oxidation and SOA formation to Indonesian peat combustion aerosols in two ways[81, 102].

The mass of SOA produced, mass of POA volatilized and, therefore, total OA enhancement (= (SOA+POA)/POA) were determined using the relative contribution of a low-volatility POA tracer to the total organic signal in dual smog chambers[81]. OA enhancement after 1.5 hr was 1.05–1.06 for

Indonesian peat combustion aerosols, and the peat smoke had a relatively low f_{44}, similar to that of coniferous-canopy smoke[81].

The Singapore group[102] identified SOA and OPOA of Lab-PM, using a potential aerosol mass reactor (Kang et al., 2007) at high and low relative humidities. As shown in Fig. S8, the experiments were conducted for three cases: POA aging, SOA formation and mixed POA aging and SOA formation. Fresh peat smoke has a relatively low f_{44} [69, 81], but the SOA formed was characterized chemically as highly oxygenated ($f_{44} > 0.15$ for most cases), and the values of both f_{60} (a marker for LG-like species) and f_{HMW} (m/z > 100, a marker for high-molecular-weight species) were significantly lower than those for POA and aged POA particles[81, 109]. It can be difficult to separate OPOA and SOA mass spectra in OOA as mentioned in Section S4.1. OPOA, however, could be differentiated from some SOA by examining the higher molecular weight species [102]. Comparing the secondary OPOA and SOA mass spectra to the OOA factor of the 2015 haze observed in Singapore suggested that the observed OOA contained a mixture of SOA and OPOA[102].

The mass fraction of sulfate in fresh Lab-PM and aged POA was below 0.6%, but the fraction increased 10 ~20% for SOA and was 0.6% for the mixed cases (Table S4). A similar increase in the mass fraction of ammonium was also observed in SOA experiments. An increase in the mass percentages of sulfate and ammonium in aged particles was observed in other laboratory experiments[83] and the 2015 haze particles in Singapore[73]. These observations coincide with the lower mass percentages of sulfate and ammonium in PM filter samples taken near fire sources (< 1%)[77, 85] and the enhanced percentages at receptor sites in field mesurements[16, 41, 73]. Ammonia is a major trace gas emitted by Indonesian peat fires in both field (Stockwell et al., 2016) and laboratory experiments (Stockwell et al., 2014). Sulfur in peat samples may enhance the mass fractions of sulfate. Data on SO_2 are limited[116], however, and gaseous precursors need to be measured before injecting the peat-combustion smoke into the reactor to unravel the mechanism of secondary aerosol formation in laboratory experiments.

S4.3 Relationship between chemical compositions and physical properties

Light-absorbing BrC constituents in haze samples and Lab-PM were characterized at the molecular level at selected wavelengths by UPLC/DAD-ESI-HRQTOFMS (see the "Appendix" sheet in the dataset) in the negative ion mode[65]. A significant number of oxygenated−conjugated species were identified in fresh peat-combustion aerosols (Lab-PM), and in the haze samples, the BrC constituents accounted for only 0.4% of the OA in the ambient $PM_{2.5}$ mass because of a lack of authentic standards[65] (Table S5). Although HULIS was observed in the IPF aerosols in field measurements[105,106] and in laboratory experiments as mentioned in Section S4.1[86], HULIS was not chromatographically resolved[65]. Four nitroaromatics that might come from vegetation burning and fossil fuels, as found in the haze samples, were not detected in the laboratory-generated aerosols [65].

The water-uptake properties of IPF aerosol particles are closely related to their aerosol-water content, optical properties and cloud activation potential through their hygroscopic growth. The Singapore group[74] employed a humidified tandem differential mobility analyzer (HTDMA) to determine the relationships between water uptake properties (diameter growth factor and hygroscopicity parameter) and the chemical compositions of the 2015 haze particles. Although laboratory experiments[23, 66] indicated that fresh peat-combustion aerosols were weakly hygroscopic, the haze particles were generally hygroscopic. This discrepancy is suggested to be due to the transformation of IPF aerosols during their transport in the atmosphere, with sulfate and SOA formation (and OOA) key in promoting the hygroscopic growth of the haze particles[74].

The dependence of WSOM polarity of Lab-PM samples on hygroscopic growth and CCN activity was investigated using water-solubility-segregated fresh [66, 82, 112] and aged [109] WSOM particles. The hygroscopic growth of the extracted WSOM particles correlated positively with polarity, and highly hydrophilic WSOM fractions contributed predominantly to this hygroscopic growth[82, 112] and CCN actvity[112]. CCN activation of WSOM in peat combustion was limited by water solubility because 44% of the WSOM consisted of less-polar/soluble compounds (solubility < 10^{-3} g cm^{-3}) and about 10% of the compounds existed in the aqueous phase at the point of activation[112].

The size and RH dependence of chemical compositions and the hygroscopicity of aged POA particles were quantified for two separate processes[109], i.e., chemical aging of POA and SOA formation (Fig. S8)[102]. Conversion from POA to OPOA was pronounced when RH in the reactor was higher, and the hygroscopicity parameter of the aged POA particles correlated linearly with the OPOA mass fraction[109]. Oxidation of fresh combustion particles is expected to proceed faster at elevated RH due to reduced viscosity following hygroscopic growth (phase shift from a likely (semi)-solid state of peat-combustion POA [23] to a liquid state), and the enhancement of hygroscopicity following oxidation is larger for smaller particles[109].

6. Size Distributions

S6.1 Total mass

In Singapore, some researchers[25, 42, 47, 48, 93] have presented size distributions on hazy and non-hazy days. Larger peaks for PM mass existed in the fine mode at (i) around 3.2 μm[25] during both haze and non-haze periods, and (ii) 0.56 – 1.0 μm during a smoke-haze period[47, 48] and 0.32 – 0.56 μm[48] or 0.18 – 0.32 μm[47] during a non-haze period in 2001–2002. Smaller peaks existed in the coarse mode at around (i) 3.2 μm[25], (ii) 3.2 – 5.6 μm during both haze and non-haze periods[48], and (iii) 1.8 – 5.6 μm during the haze period and 1.8 – 3.2 μm during non-haze periods[47]. Although the mass concentration in the fine mode is considerably higher than that in coarse mode during both periods, a larger increase (nearly doubled) in coarse particles than in fine particles was observed during the haze period [25]. The

authors suggest that the larger increase in coarse particles is due to the agglomeration of fine particles during long-range transport[25], but the enhancement in coarse-mode particles is also considered to be from mineral dust particles suspended during the wildfire period[118]. It is essential to know the chemical compositions, particularly of the crustal elements in the coarse mode. In other field measurements, significant increases in PM mass in the accumulation mode were observed[48]. Measurement using a four-stage cascade impactor (< 2.5 μm) indicated that the increase in particle mass in the size range of 0.2 –1.0 μm during haze periods was relatively higher compared to that of quasi ultrafine particles (< 0.2 μm)[42].

According to SMPS and APS measurements, bimodal number distributions were found with peaks at approximately 0.01 μm and 0.035 μm on clear days, and 0.05 μm and 0.4 μm on hazy days. The total number concentration of 8 nm to 20 μm particles was elevated to 5.31×10^5 cm^{-3} on hazy days (about twofold compared to clear days) [25]. FMPS measurements in 2009 revealed that total number concentration during hazy days was comparable to that during non-hazy days across the entire size range (5.6 – 560 nm) but was higher (about twofold) than that during non-haze days in the size range of 101 – 560 nm[53]. In combination with samplings of cascade impactor and SEM observations, the larger particles ($PM_{8.1-20}$) were irregularly shaped, while the smaller particles ($PM_{2.0-4.0}$ and $PM_{0.25-0.5}$) formed aggregates of pseudo-spherical morphology[93]. Moreover, the smaller PM ($PM_{0.25-0.5}$) during the hazy periods also showed crystal-like structures.

In Thailand, size distributions were determined by Nano sampler[92, 119]. This sampler separates particles into $PM_{<0.1}$, $PM_{0.1-0.5}$, $PM_{0.5-1}$, $PM_{1-2.5}$, $PM_{2.5-10}$ and $PM_{>10}$. Haze samples in 2015 showed a bimodal distribution. The majority of particles were in the accumulation mode with a mean particle size of 0.75 μm, and a much smaller peak at 4.0 μm was observed in the coarse mode[92]. During partial and strong haze periods in 2019, PM_1 was the predominant component (45.1 and 52.9% in TSP mass concentrations in partial and strong haze periods, respectively, and 34% in normal period), and the highest PM mass contribution was in the $PM_{0.5-1.0}$ size range[119]. No clear differences in $PM_{0.1}$ mass fractions were observed at any time during the year.

Size distributions have been measured for PM emissions from smoldering (or natural) combustion of Indonesian peat using a five-stage (Berner type) cascade impactor (Table S9) in laboratory experiments[23, 26]. In an experiment by Iinuma et al.[26], PM EFs were determined, and the unimodal mass size distribution showed dominance of larger particles, peaking at Stage 3 followed by Stage 4. Dusek et al.[23] also observed unimodal number size distribution with a peak of 0.15 μm measured by DMA+CPC, and roughly 40% of the particles found in the SEM images in the 0.1 to 1 μm size range were hollow spheres. In addition, their measurements using a CCN counter demonstrated that peat smoke particles were not activated to cloud droplets at high supersaturation (1.6%), and these hydrophobic particles were present predominantly in the size range of larger than 0.2 μm.

S6.2 Chemical species

In Singapore, size distributions of elemental components in IPF-derived haze periods were reported. Orlic et al.[4] measured 24 elemental concentrations in PM during normal and haze periods in 1994, using a six-stage cascade impactor (the later four stages and backup filter were used for PIXE analysis). The elemental size distributions in haze periods, however, were not presented, and only typical distributions were shown. The authors mentioned that the average concentrations of S, K, Ti, V, Mn, Ni, As and Pb during haze periods were three to six times higher than those during normal periods. Twenty-four elements in 12 different size fractions (10 nm – 10 μm) were determined during haze and non-haze periods in 2012 with MOUDI and NanoMOUDI samplers and ICP-MS analysis[47]. The ratios of elemental concentrations measured between a smoke haze episode and a non-haze period varied from 1.2 (Bi) to 6.6 (Co) in coarse ($PM_{2.5–10}$), fine ($PM_{2.5}$), ultrafine ($PM_{0.01–0.1}$), and nano ($PM_{0.01–0.056}$) particles. The elemental concentrations across the entire size range showed higher levels during the haze episode than during the non-haze period. The fine mode accounted for the largest share in total elemental concentration for all elements during both periods. Three distinct patterns of size distributions of elemental concentrations were identified as follows: (i) elements concentrated in the coarse mode (Al, Ba, Ca, Fe, Mg and Sr), (ii) elements concentrated in the accumulation mode (Cd, Ni, Pb, Se, Te and Tl), and (iii) the remaining elements (B, Be, Bi, Co, Cr, Cu, Ga, K, Li, Mn, Na and Zn) showing multimode distributions.

In Thailand, mass size distributions of carbonaceous components in PM[96] and PM-bound PAHs[119] were measured using a Nano sampler. Phairuang et al.[96] determined size-segregated OC and EC concentrations throughout 2018, including the period of transboundary haze from Indonesia (June – August) in southern Thailand. They suggested that transported plumes from Indonesian forest fires may have increased the OC and EC concentrations in both the fine mode ($PM_{0.5-1.0}$ and $PM_{1.0-2.5}$) and coarse mode ($PM_{2.5-10}$ and $PM_{>10}$) fractions. The OC fraction in $PM_{0.1}$ was also shown to be significantly affected by the plumes during the pre-monsoon season (May – August). Mahasakpan et al.[119] measured the size distributions of PM-bound PAHs, employing a Nano sampler at a background site in Thailand in 2019, including periods of partial and strong transboundary haze from Indonesia. As shown in Table S10, the total PAH concentrations in PM_1 and $PM_{2.5}$ during a strong haze period were five to sixfold higher than those during a normal period. The total PAH concentrations in PM_1 and $PM_{0.1}$ accounted for 69% and 11% of those in $PM_{2.5}$, respectively. The average BaP concentration in $PM_{2.5}$ during the strong haze period increased tenfold compared to that during the normal period, and the share of PM_1 in $PM_{2.5}$ was roughly 70% according to a figure in the literature[119]. These findings indicate that PM_1 was the major fraction in terms of particle-bound PAHs during the haze period.

Mass size distributions of chemical species were reported in the two laboratory experiments described in Section S6.1. Dusek et al.[23] determined the size distributions of inorganic ions, EC, OC, WSOC and WIOC (= TC–WSOC). In Stage 1, carbonaceous components were dominant, and WSOC and WIOC accounted for about 33% and 6% of total mass concentrations, respectively. However, WSOC and WIOC contributed 13% and 31% of total mass, respectively in Stage 2. The contributions of inorganic ions were less than 2% in both stages, and the mass contributions by chemical species in other stages were not shown. Iinuma et al. [26] presented mass size distributions of carbonaceous components, inorganic ions and organic compounds based on their EFs. WIOC was dominant in TC in stages 2 to 4, while WSOC was massive and WIOC was not detected in stages 1 and 5 (Table S11). They determined the size-resolved EFs of carbonaceous components (EC, OC, WSOC, WIOC = OC–WSOC), eight inorganic ions and 89 organic compounds (n-alkanes, n-alkenes, PAHs, OPAHs, lignin decomposition products, nitrophenols, resin acids and decomposition products of cellulose and hemicellulose). The mass size distributions of typical species based on their EFs are shown in Table S12. All species were classified into four types of distributions: three types of unimodal distributions, peaking (gray shaded part in Table S12) in (i) Stage 3 (0.42 – 1.2 μm), (ii) Stage 4 (1.2 – 3.5 μm), and (iii) Stage 1 (0.05 – 0.14 μm), and one type of bimodal distribution, peaking in (iv) Stage 1 and Stage 3 (or 4). The components included were type (i) carbonaceous components, organic compounds except total n-alkanes, and inorganic ions ($Mg^{2+}$and Ca^{2+}); type (ii) total n-alkanes and the remaining three inorganic ions (NO_3^-, SO_4^{2-} and K^+); type (iii) NH_4^+; and type (iv) Na^+, Cl^- and WSOC. Potassium ions had a sharp unimodal distribution with the mass being concentrated in Stage 4. The EFs in Stages 3 and 4, however, were comparable for n-alkanes and n-alkenes, and some species showed broad distributions. Lower size resolution of the impactor may produce an apparent unimodal distribution by smoothing bimodality.

Supplementary References

Kang, E., Root, M.J., Toohey, D.W. and Brune, W.H. (2007) Introducing the concept of Potential Aerosol Mass (PAM). *Atmospheric Chemistry and Physics,* 7: 5727–5744.

Kuwata, M. and Lee, W.-C. (2017) 1-octanol-water partitioning as a classifier of water soluble organic matters: Implication for solubility distribution. *Aerosol Science and Technology*, 51: 602−613.

McNeill, V.F. (2015) Aqueous organic chemistry in the atmosphere: Sources and chemical processing of organic aerosols. *Environmental Science & Technology*, 49: 1237−1244.

Stockwell, C. E., Jayarathne, T., Cochrane, M.A., Ryan, K.C., Putra, E.I., Saharjo, B.H., Nurhayati, A.D., Albar, I., Blake, D.R., Simpson, I.J., Stone, E.A. and Yokelson, R.J. (2016) Field measurements of trace gases and aerosols emitted by peat fires in Central Kalimantan, Indonesia,

during the 2015 El Niño. *Atmospheric Chemistry and Physics,* 16: 11711–11732.

Stockwell, C.E., Yokelson, R.J., Kreidenweis, S.M., Robinson, A.L., DeMott, P.J., Sullivan, R.C., Reardon, J., Ryan, K.C., Griffith, D.W.T. and Stevens, L. (2014) Trace gas emissions from combustion of peat, crop residue, domestic biofuels, grasses, and other fuels: configuration and Fourier transform infrared (FTIR) component of the fourth Fire Lab at Missoula Experiment (FLAME-4). *Atmospheric Chemistry and Physics*, 14: 9727–9754.

List of Tables and Figures in Supplementary Information

Fig. S1 Mass concentrations of water-soluble inorganic ions in fine particles ($PM_{2.5}$ or less) during haze and non-haze periods.

Fig. S2 Mass percentages of water-soluble inorganic ions in fine particles ($PM_{2.5\ or\ less}$) during haze and non-haze periods.

Fig. S3 Mass concentrations of major elements in fine particles ($PM_{2.5\ or\ less}$) during haze and non-haze periods.

Fig. S4 Mass fractions of major elements in fine particles ($PM_{2.5\ or\ less}$) during haze and non-haze periods, and in laboratory-generated fresh smoke particles.

Fig. S5 Mass concentrations and mass fractions of 16 PAHs in PM (TSP, PM_{10} and $PM_{2.5}$) in PM during haze and non-haze periods. These data were obtained from the following studies: (upper) [24, 28, 37, 43, 51, 70, 72, 73, 82, 88, 119] and (lower) [26, 28, 37, 43, 72, 77, 92, 119].

Fig. S6 PAH diagnostic ratios for PM. The data were obtained from the following studies: (A) [13, 24, 28, 37, 43, 51, 70, 108], (B) [13, 28, 37, 43, 51, 88, 92, 108], (C) [13, 28, 37, 43, 51, 77, 88, 92, 108].

Fig. S7 Four source factors of OA identified in NR-PM_1 (haze particles) by ToF-ACSM.

Fig. S8 Laboratory experimental system for separating POA aging (OPOA), SOA formation, and mixed POA aging and SOA formation[102, 109]. (Individual experiments performed by switching the corresponding valve.)

Table S1 Summary of the review papers including properties of haze from peatland fires in Southeast Asia.

		Radojevic, 2003	Hu, et al., 2018	Latif, et al., 2018	Istiqomah & Marleni, 2020	Adam, et al., 2021	Daharai, et al., 2021	Fujii & Tohno, 2021	Saksakulkrai, et al., 2022	Van, et al., 2022	This study
	Lit. No.	19	75	78	94	99	103	104	113	116	
Phenomena	Ambient PM pollution				○		○		○		
	Haze by peatland (forest) fires	○	○	○	△	○	△	○	△	○	○
	Haze by other BB emissions (agriculture waste burning, etc.)			○	△	○	△		△	○	
Lab. study (peat fire emissions)	Combustion		Smoldering								
	Peat		Boreal, tempearte, tropical peats					Indonesian and Malaysian peats			Indonesian and Malaysian peats
Country	Indonesia	○	○		○	○	○	○	○	○	○
	Brunei	○							○		○
	Malaysia	○		○		○	○	○	○	○	○
	Singapore	○				○	○	○	○	○	○
	Thailand					○	○		○	○	○
	Vietnam					○	○		○	○	
	Phillipines								△		
	Myanmar								△		
	Cambodia								△		
	Laos								△		
Emission factor			○					○			○
Physical and chemical characteristics of PM (haze)	Total mass concentration	○	Total mass	○	○	○	○	○	○	○	○
	Total number concentration					○	○				△
	AOD					○					
	Size distribution					○					○
	EC (BC)	○	○	○	○	○	○	○	○	○	○
	OC	○	○	○		○	○	○	○	○	○
	WSOC					○		○			○
	HULIS							○			○
	BrC					○		○			○
	Metals	○		○	○	○	○	○	○	○	○
	Other elements	○		○	○	○	○	○	○	○	○
	Water--soluble inorganic ions	○		○	○	○	○	○	○	○	○
	Organic compounds	○	○	LG, MN, GL, CHL, DA		○	○	○	LG, MN, GL	LG	○
	Aerosol mass spectra analysis										○
	PAHs	○	○	○		○	○	○	△	○	○
	SIA formation								○	○	○
	SOA formation								○	○ *	○
	Isotopes										○
	Hygroscopicity					○					○
Rainwater composition		○		○							
Gaseous species		○	○							○	
Haze impact	Climate	○				○					
	Health		○	○		○	○			○	
	Economy			○						○	
	Others			○		○					
Source apportionment				○	○	○	○	○	○	○	○
Policy						○				○	
Publication year of articles		1991-2000	1997-2018	1996-2018	2008-2019	2010-2020	1997-2017	1998-2021	2002-2022	1989-2022	1993-2023

LG: Levoglucosan, MN: Mannosan, GL: Galactosan, CHL: Cholesterol, DA: Dehydroabietic Acid
△: Available data is limited (e.g., chemical compositions are not available.)
* Studies relating to SOA in haze periods in Southeast Asia have not been considered yet.

Table S2 Search queries and numbers of extracted articles.

Database	Search string	Extracted articles (identified ones)
Web of Science	ALL=("particulate matter*" OR PM OR PM10 OR PM2.5 OR TSP OR haze OR aerosol) **AND** ALL=(peat* OR fire OR "biomass burning") **AND** ALL=(Indonesia OR Kalimantan OR Sumatra OR Malaysia OR Singapore OR ASEAN OR "Southeast Asia") **AND** ALL=(chemical* OR component* OR composition* OR PAH* OR carbonaceous* OR elemental* OR inorganic* OR organic* OR EC OR OC OR "Brown carbon" OR WSOC OR HULIS* OR SOA* OR ions OR metal* OR "trace element*" OR "heavy metal*")	92 (607)
Scopus	TITLE-ABS-KEY ("particulate matter" OR PM* OR TSP OR haze OR aerosol) **AND** TITLE-ABS-KEY (peat* OR fire OR "biomass burning") AND TITLE-ABS-KEY (Indonesia OR Kalimantan OR Sumatra OR Malaysia OR Singapore OR Brunei OR ASEAN OR "Southeast Asia") **AND** TITLE-ABS-KEY (chemical* OR component* OR composition* OR PAH* OR carbonaceous* OR elemental* OR inorganic* OR organic* OR EC OR OC OR "Brown carbon" OR WSOC OR Hulis* OR SOA* OR ions OR metal* OR "trace element" OR "heavy metal")	100 (519)
ScienceDirect	("particulate matter" OR haze) **AND** (peat OR "biomass burning") **AND** (Indonesia) **AND** (chemical OR composition OR characterization)	30 (643)
Screened articles by snowballing		13
Final screened articles		121
Review articles		9
Newly published article after screening was over		1
Final screened articles excluding review ones		113

Table S3 Chemical species corresponding to polarity of WSOM in laboratory-generated aerosols from Indonesian peat combustion[86]. Following water extraction of the filter samples, 1-octanol-water extractions were conducted for five volume ratios of the 1-octanol and aqueous phases. Polarity-segregated aerosols were generated by nebulizing the aqueous solutions [66, 82, 109, 112] and octanol-phase solutions diluted by methanol [82, 109, 112].

Polarity of WSOM	Chemical species
Highly polar fraction	Highly oxygenated and similar optical properties as those of light-absorbing humic-like substances (HULIS)
Marginally polar fraction	Mostly consisted of hydrocarbon-like and high molecular weight species
The least-polar fraction	Aromatic compounds

Table S4 Mass percentages of major inorganic species in field samples and laboratory-generated aerosol particles. (Measurements conducted by ToF-ACSM and IC.)

Sample (measurement method)	PM	Mass percentage	Literature No.
Ambient aerosols (ToF-ACSM)	NR-PM_1 during 2015 haze episode in Singapore	SO_4^{2-} ~12%, OA ~80%,	73
Laboratory-generated aerosols from Indonesian peat burning (ToF-ACSM)	NR-PM_1 (Fresh particles)	Total inorganic species < 1% (NO_3^{-*} ~0.6%, SO_4^{2-*}: ND, NH_4^+ ~0.2%) , OA ~99%,	65
	NR-PM_1 (POA aging)	SO_4^{2-}: ND	102
	NR-PM_1 (SOA formation)	SO_4^{2-} ~10%	102
		SO_4^{2-} ~21%, NH_4^+ ~15%	109
	NR-PM_1 (mixed)	SO_4^{2-} ~0.6%, NH_4^+ ~0.9%	109
Laboratory-generated aerosols from Malaysian peat burning (Ion chromatography, IC)	$PM_{2.5}$ (fresh)	SO_4^{2-} ~0.56%, NH_4^+ ~0.002%	83
	$PM_{2.5}$ (aged, 2d)	SO_4^{2-} ~0.17%, NH_4^+ ~0.83%	83
	$PM_{2.5}$ (fresh)	SO_4^{2-} ~0.13%, NH_4^+ ~0.003%	83
	$PM_{2.5}$ (aged, 7d)	SO_4^{2-} ~1.96%, NH_4^+ ~7.74%	83

* Partly from fragments from thermal decomposition of organonitrates and organosulfates

Table S5 Characterized BrC OA constituents that absorb in the near-UV and visible wavelengths region (365, 400, 500, and 580 nm) [65].

Sample	Identified BrC OA constituents	Mass percentage of the constituents in OA
Laboratory-generated aerosols from Indonesian peat burning	Number of species (41) 19 (365 nm), 2 (400 nm), 9 (500 nm), 11 (580 nm) Tentatively assigned most abundant constituents · Vanillin, ferulic acid and homovanillic acid (365 nm) · Ethyl guaiacol, coniferyl aldehyde, coniferyl alcohol (visible wavelengths) Oxygenated−conjugated compounds (99.4% of the total quantified BrC OA species) and trace amounts of N- and S-containing compounds	16%
$PM_{2.5}$ sampled during the 2015 haze episode in Singapore	Number of species (10) 6 (365 nm), 0 (400 nm), 3 (500 nm), 1 (580 nm) and 4 nitroaromatics (from vegetation burning and fossil fuels?) Tentatively assigned most abundant constituents · Ferulic acid, p-coumaric acid, coniferyl aldehyde	0.4%

Table S6 Summary of indicators of Indonesian peatland fire aerosols (field observations).

Lit. No.	Location	Country	PM size	OC, EC analysis	Remarks	OC/EC	OP/OC4	(OC2+OC3+OP) /soot-EC	char-EC /soot-EC	WSOC/OC	WSOC/TC	HULIS-C /OC	HULIS-C /WSOC	MN/LG	SA/LG	V/LG	SA/VA
5	Palembang Sriwijaya University	Indonesia	$PM_{2.5}$ $PM_{2.5}$	Thermo-optical analysis		52.2 62.5											
7	Pulau Seibu Serpong Singapore	Indonesia (2 sites, major haze was over) Singapore (1 site, thick haze)	$PM_{2.1}$	Elemental analyzer (TC)	3 sites average BKG						0.29 (0.05- 0.32) 0.16						
28	Sungai Sembilan Belakang Rumah Pekanbaru	Indonesia	$PM_{2.5}$	CHN analyzer (EC: >350°C)	Sungai Sembilan Belakang Rumah Pekanbaru	2.42 2.09 1.43											
49	Sepahat Village (fire site) Sukajadi Village (Riau, Sumatara, background)	Indonesia	$PM_{2.5}$	TOR IMPROVE_A	Seven fire sites Four BKG sites (Lit. 44)	36.4 ± 9.08 2.99 ± 0.738								0.098 ± 0.021 0.072 ± 0.017	0.079 ± 0.023	0.0074	0.96 ± 0.14
45	Palangkaraya in Central Kalimantan (urban) Taruna in Central Kalimantan (rural)	Indonesia	PM_{10}		Urban Rural	14.8 5.68											
63	Central Kalimantan (Fresh smoke emissions from smoldering fires)	Indonesia	$PM_{2.5}$	TOT NIOSH5040	7 plume-samples	77.4± 35.5											
77	Palangka Raya	Indonesia	$PM_{2.5}$	TOT NIOSH5040	2–3 m downwind of the smoldering peat	67±26				0.16±0.11				0.021 ± 0.010	0.088 ± 0.11	0.00065	0.48 ± 0.13
89	Jambi	Indonesia	$PM_{2.5}$	TOR IMPROVE_A		20.4 ± 8.7	0.9 ± 0.2	54.7 ± 19.9	2.8 ± 1.9								
101	Padang, Jambi, and Pekanbaru	Indonesia	Nano sampler $PM_{0.1}$, $PM_{0.5\text{-}1}$, $PM_{1\text{-}2.5}$ $PM_{2.5\text{-}10}$, $PM_{>10}$	TOR IMPROVE	Penkanbaru $PM_{0.1}$ $PM_{2.5}$ PM_{10} TSP Penkanbaru $PM_{0.1}$ $PM_{2.5}$ PM_{10} TSP	4.5 4.9 4.6 4.6 5.4 4.4 3.9 3.9											
106	Siak, Kampar	Indonesia		TOR IMPROVE_A	All Siak Kampar	209 ± 188 223 ± 120 186 ± 283	2.99 ± 2.58 - -	44.3 ± 22.0 - -	0.453 ± 1.11 - -	0.085 ± 0.015 0.089 ± 0.015 0.079 ± 0.015		0.054 - -	0.55 ± 0.085 - -	0.091 ± 0.023 0.095 ± 0.025 0.076 ± 0.012	0.045 ± 0.0075 0.042 ± 0.0077 0.049 ± 0.0057		0.52 ± 0.43 0.33 ± 0.18 0.81 ±0.57

115	Pekanbaru	Indonesia	Coarse: $PM_{2.5-10}$ Fine: $PM_{2.5}$	TOR IMPROVE	$PM_{2.5}$	3.02									
2	Petaling Jaya	Malaysia	TSP	TOR (laser-combustion method)	Haze Non-haze	8.2 1.75									
5	Petaling Jaya	Malaysia	$PM_{2.5}$	Thermo-optical analysis		13.7									
18	Petaling Jaya Gombak	Malaysia	$PM_{2.5}$	TC: thermal decomposition (850°C) EC: integrating plate method OC=TC-EC	**Excessive haze** Petaling Jaya **Excessive haze** Gombak	3.05 2.24									
21	Kuala Lumpur	Malaysia	TSP	TOR (laser-combustion method)		13 ± 4.5									
50	Petaling Jaya	Malaysia	$PM_{2.5}$	TOR IMPROVE_A	SW monsoon Annual	3.3 ± 1.5 2.3 ± 1.2	2.5 ± 3.3 1.0 ± 2.2	230 ± 270 140 ± 180	110 ± 120 91 ± 91			0.053 0.056	0.0022 0.0029	0.01	0.90 1.32
56	Bangi	Malaysia	TSP	TOR IMPROVE_A	Strong haze Light haze Non-haze	9.81 ± 0.40 4.16 ± 0.62 2.53 ± 0.75	12.7 ± 1.02 5.29 ± 1.23 0.18 ± 0.29	9.07 ± 0.29 3.72 ± 0.61 2.04 ± 0.69	12.2 ± 2.89 18.0 ± 5.87 23.4 ± 12.31			0.12 0.113 ± 0.015 0.108 ± 0.014	0.021 0.031 ± 0.001 0.050 ± 0.009	0.0087	0.77 1.04 ± 0.034 1.07 ± 0.072
57	Bangi	Malaysia	$PM_{2.5}$	TOR IMPROVE_A	Haze	2.69 ± 0.935									
61	Kuala Lampur	Malaysia	$PM_{2.5}$	TOR IMPROVE_A	SW monsoon	2.97 (0.55 - 11.2)									
88	Kuala Lampur	Malaysia		-	Haze							0.085			
105	Bangi	Malaysia	TSP	TOR IMPROVE_A	Strong haze Light haze Non-haze	34 (ave.) 39 ± 3.4 -				0.34 (ave.) 0.39 ± 0.034 0.41± 0.064	0.73 (ave.) 0.71 ± 0.033 0.52 ± 0.16				
111	Kuala Lumpur	Malaysia	Nano sampler $PM_{0.1}$, $PM_{0.5-1}$, $PM_{1-2.5}$ $PM_{2.5-10}$, $PM_{>10}$	TOR IMPROVE	**TSP** NE monsoon Intermonsson 1 SW monsoon Intermonsson 2 **$PM_{0.1}$** NE monsoon Intermonsson 1 SW monsoon Intermonsson 2	3.33 3.26 2.96 4.39 6.96 ± 1.27 4.67 ± 0.59 3.61 ± 0.24 5.59 ± 0.84 4.84 ± 0.46 (All)			- 0.61 ± 0.23 0.66 ± 0.15 0.83 ± 0.08 1.69 ± 0.68 0.67 ± 0.07 (All)					
16	National University of Singapore	Singapore	$PM_{2.5}$	CHN 2400 analyzer TC, IC (1M HCl) EC (resultant mass after 350°C for 24 h) OC = TC–IC–EC	May haze Haze	6.03 ± 3.07 3.25				0.30 ± 0.10					
25	National University of Singapore Kent Ridge campus	Singapore	$PM_{2.5}$	TOR or TOT IMPROVE CHN 2400 analyzer	Hazy Clear	2.79 1.99									

29	National University of Singapore	Singapore	TSP	-	Haze							1.39
				-	Non-haze							0.99
43	Tropical Marine Science Institute on St. John's Island	Singapore	TSP	TOT (Modified NIOSH)	Haze	15.5					0.1	
					Clear	2.6					0.3	
73	Nanyang Technological University	Singapore	$PM_{2.5}$	TOR IMPROVE_A	Haze	4.75				0.64		
74	Nanyang Technological University	Singapore	$PM_{2.5}$	TOR IMPROVE_A	Haze	3.99				0.636 ±0.073		
89	National University of Singapore	Singapore	$PM_{2.5}$	TOR IMPROVE_A	Non-smoke nighttime	1.8 ± 0.6	2.3 ± 0.6	1.9 ± 0.4	0.21 ± 0.17			
					Non-smoke	2.3 ± 1.0	2.1 ± 1.2	3.6 ± 3.6	1.0 ± 1.6			
					Smoke	4.8 ± 2.5	2.3 ±1.6	13.4 ± 11.6	4.1 ± 5.6			
					Episodic smoke	14.9 ± 2.9	4.8 ± 0.5	20.1 ± 4.1	0.59 ± 0.64			
107	National University of Singapore	Singapore	$PM_{2.5}$	TOR IMPROVE_A	Smoke dominant	13			8.2 (2011) 2.3 (2015) 3.8 (2019)			
96	Hat Yai	Thailand	$PM_{0.1}$ $PM_{0.5-1}$ $PM_{1-2.5}$ $PM_{2.5-10}$ $PM_{>10}$ TSP	TOR IMPROVE	**Annual ave.** $PM_{0.1}$ $PM_{0.5-1}$ $PM_{1-2.5}$ $PM_{2.5-10}$ $PM_{>10}$	2.91 3.06 3.78 4.30 3.80			0.36 1.15 1.40 2.02 1.09			
			$PM_{0.1}$		Dry Pre-Monsoon Monsoon	2.44 3.29 3.00			0.36 0.31 0.40			
120	Hat Yai	Thailand	$PM_{2.5}$	TOR IMPROVE	Haze	4.7				0.4		
					Non-haze	2.8 ± 0.1				0.5 ± 0.1		
122	Thepha beach	Thailand	$PM_{2.5}$	TOR IMPROVE	Normal	3.8 ± 1.2				0.5 ± 0.2		
					Partial haze	1.8 ± 0.1				0.5 ± 0.1		
					Strong haze	5.2 ± 2.5				0.4 ± 0.1		
	Songkhla Community College				Normal	2.7 ± 0.7				0.5 ± 0.2		
					Partial haze	1.7 ± 0.3				0.6 ± 0.1		
					Strong haze	3.3 ± 0.5				0.4 ± 0.2		
	Wang Yai Sub-district				Normal	3.3 ± 0.7				0.5 ± 0.2		
					Partial haze	1.9 ± 0.1				0.6 ± 0.2		
					Strong haze	4.2 ± 1.3				0.5 ± 0.02		
	Pattani city				Normal	3.0 ± 0.9				0.5 ± 0.1		
					Partial haze	2.0 ± 0.4				0.7 ± 0.2		
					Strong haze	3.8 ± 0.6				0.5 ± 0.2		

Table S7 Summary of indicators of Indonesian peatland fire aerosols (laboratory experiments).

Lit. No.	Peat	PM size	OC, EC analysis	Remarks	OC/EC	OP/OC4	(OC2+OC3+OP) /soot-EC	char-EC /soot-EC	WSOC/OC	WSOC/TC	HULIS-C /OC	HULIS-C /WSOC	MN/LG	SA/LG	V/LG	SA/VA
17	Indonesian peat (south Sumatra) mosisture 30.5%	$PM_{2.5}$			151											
23	**Indonesian peat** ~10% water content	0.05 -10 μm	Thermographic method	50 - 140 nm (stage 1) 140 - 420 nm (stage 2)					0.87 0.30							
26	**Indonesian peat** ~11% water content	0.05 -10 μm	Thermographic method (C-mat 5500)		14				0.39				0.088	0.044	0.014	9.17
66	**Indonesian peat** (Riau,Sumatra & Palangkaraya, Central Kalimantan(CK))	Nebulizing aqueous solutions containing extracted WSOM from filter samples	TOR IMPROVE_A	**Riau peat** Drained and burnt area Secondary forest Undisturbed area **CK peat** Drained and unburnt area Drained and burnt area	98-145 109 86 112 150				0.0093 - 0.0180 0.0415 0.0608 0.0416 0.0203							
83	**Malaysian peat** (Borneo) 25% fuel moisture	$PM_{2.5}$	TOR IMPROVE_A	Fresh Aged (~2 d) Fresh Aged (~7d)	96.5 34.1 49.5 85.9	2.46 2.87 1.24 2.37	11.46 9.71 11.67 7.7		0.18 ± 0.014 0.31 ± 0.081 0.21 ± 0.035 0.40 ± 0.079				0 0 0.043 0.032			
90	**Malaysian peat** (Borneo) 26% fuel moisture	$PM_{2.5}$	TOR IMPROVE_A	Fresh Aged (~2 d) Fresh Aged (~7d)	97.3 33.9 49.6 85	2.45 1.45 1.88 2.35	11.41 9.73 11.63 9.82		0.188 0.314 0.211 0.399				0 0 0.041 0.033			
95	**Indonesian peat** (Kubu Raya, western art of Kalimantan) moisture: 12.9 ± 1.5%	$PM_{2.5}$	TOR IMPROVE_A	All Surface Subsurface	132 ± 68 163 ± 55 101 ± 70	4.1 ± 4.1 5.8 ± 5.3 2.4 ± 1.4	27.2 ± 18.4 34.8 ± 21.2 19.7 ± 12.9									

Table S8 Summary of size-segregated samples and measurement of size distribution in the dataset.

Size segregation	Measurement	Online/ Offline	Size distribution	Number of articles
$PM_{2.5}$	Mass	OFF		56
$PM_{2.1}$	Mass	OFF		1
PM_{10}	Mass	OFF		11
TSP	Mass	OFF		18
Filter sampling*	Mass	OFF		12
NR-PM_1 (AMS)	Mass	ON		11
Fine: PM_2 Coarse: $PM_{2\text{-}10}$	Mass	OFF		1
Fine: $PM_{2.5}$ Coarse: $PM_{2.5\text{-}10}$	Mass	OFF		7
Fine: $PM_{1.5}$ Coarse: $PM_{1.5\text{-}100}$	Mass	OFF		1
Cascade impactor	Mass	OFF	○	7
Nano sampler	Mass	OFF	○	6
Single particle (TEM-EDS)**	Mass	OFF		3
DustTrack	Mass	ON	○	1
SMPS, DMA+CPC, FMPS	Number	ON	○	7
OPC	Number	ON	○	2
APS	Number	ON	○	1

AMS: Aerosol Mass Spectrometer
DMA: Differential Mobility Classifier
FMPS: Fast Mobility Particle Sizer
APS: Aerodynamic Particle Sizer
SMPS: Scanning Mobility Particle Sizer
CPC: Condensation Particle Counter
OPC: Optical Particle Counter

* Size data is not available
** Sampling by cascade impactor

Table S9 PAHs concentrations in three PM fractions in 2019 at a background site in Thailand[119].

Species	Particle size	Concentration (ng m^{-3})		
		Normal period	Partial haze	Strong haze
Total PAH	$PM_{0.1}$	0.11 ± 0.01	0.15 ± 0.03	0.28 ± 0.02
	PM_1	0.34 ± 0.03	0.70 ± 0.05	1.75 ± 0.13
	$PM_{2.5}$	0.43 ± 0.04	0.90 ± 0.06	2.52 ± 0.19
BaP	$PM_{0.1}$	Graphical data only		
	PM_1			
	$PM_{2.5}$	0.009	0.052	0.095

Table S10 Cutoff sizes of five-stage (Berner type) impactor.

Stage	Cutoff diameter (μm)
1	0.05 – 0.14
2	0.14 – 0.42
3	0.42 – 1.2
4	1.2 – 3.5
5	3.5 – 10

Table S11 Mass percentage of carbonaceous components in TC (assembled from the literature[26]).

Component	Mass percentage in TC (%)					
	Stage 1	Stage 2	Stage 3	Stage 4	Stage 5	Total
WSOC	86	30	25	34	100	36
WIOC	ND	63	69	60	ND	57
EC	14	7	6	6	ND	7

Table S12 Size distributions of typical components based on their PM emission factors from Indonesian peat combustion (created from the Supplemental Information in the literature[26]).

Component	$\Delta EF/\Delta log(D_p)$ (mg kg^{-1})				
	Stage 1	Stage2	Stage 3	Stage 4	Stage 5
	0.05 – 0.14 (μm)	0.14 – 0.42 (μm)	0.42 – 1.2 (μm)	1.2 – 3.5 (μm)	3.5 – 10 (μm)
Cl^-	11.4	7.94	31.2	45.2	10.1
NO_3^-	ND	2.71	7.20	32.27	5.92
SO_4^{2-}	ND	ND	11.1	17.0	6.36
Na^+	15.9	4.84	10.8	34.4	11.8
NH_4^+	1.25	ND	ND	ND	ND
K^+	ND	ND	ND	25.8	2.19
Mg^{2+}	2.24	2.13	9.61	5.59	1.25
Ca^{2+}	16.1	16.5	31.2	25.8	11.4
EC*	215	252	480	301	ND
OC*	1364	3445	7540	4689	658
WSOC*	1364	1123	2017	1678	658
WIOC*	ND	2323	5523	3011	ND
n-alkanes (total)	44.7	230	355	394	0
n-alkenes (total)	7.83	42.6	93.7	92.5	0
PAHs (total)	2.68	6.97	22.1	13.8	0
Lignin Decomposition Products (total)	76.0	333	632	314	11.4
3-Hydroxy-4-methoxybenzoic acid	20.8	77.4	177	86.0	3.07
Syringic acid	15.9	38.8	101	79.6	2.85
Levoglucosan	559	968	2642	1226	74.6
Mannosan	62.6	85.2	233	105	ND

* mgC kg^{-1} EF: Emission factor

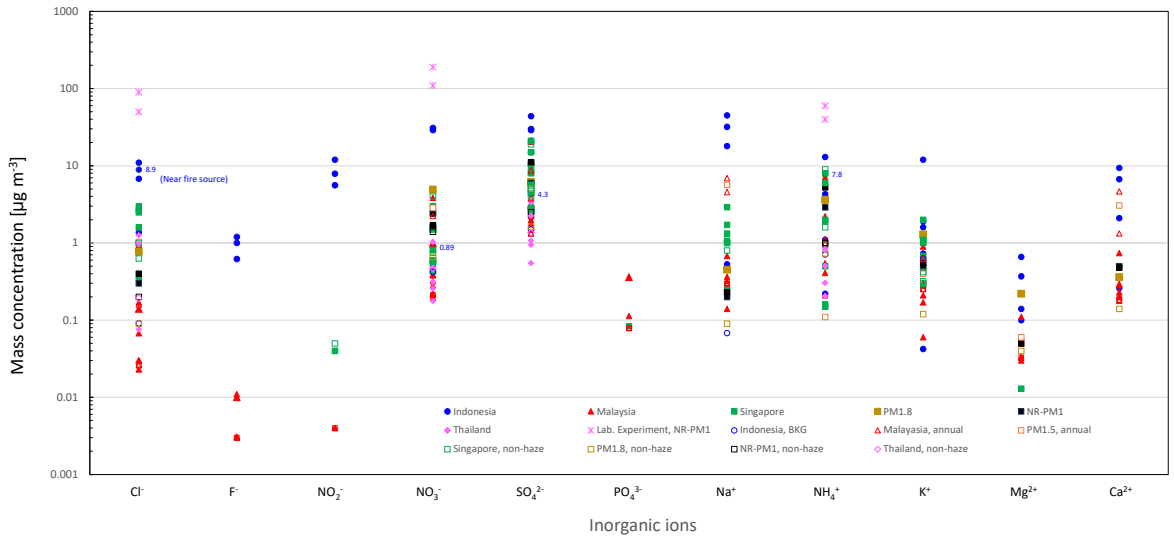

Fig. S1 Mass concentrations of water-soluble inorganic ions in fine particles ($PM_{2.5}$ or less) during haze and non-haze periods.

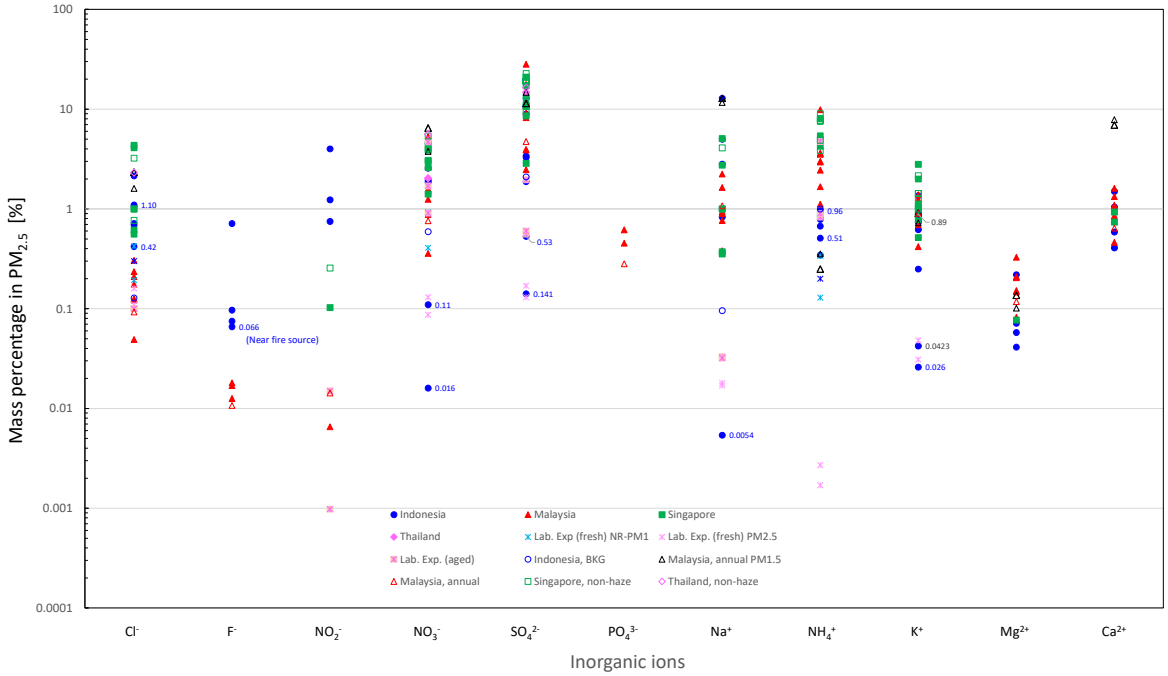

Mass percentages of water-soluble inorganic ions in fine particles ($PM_{2.5\ or\ less}$) during haze and non-haze periods.

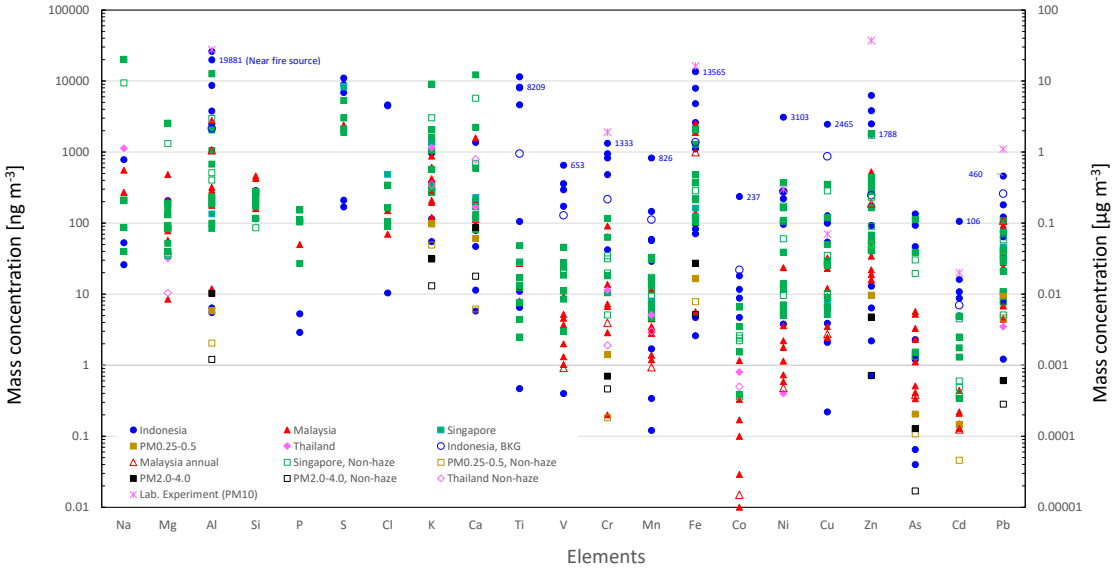

Fig. S3 Mass concentrations of major elements in fine particles ($PM_{2.5\ or\ less}$) during haze and non-haze periods.

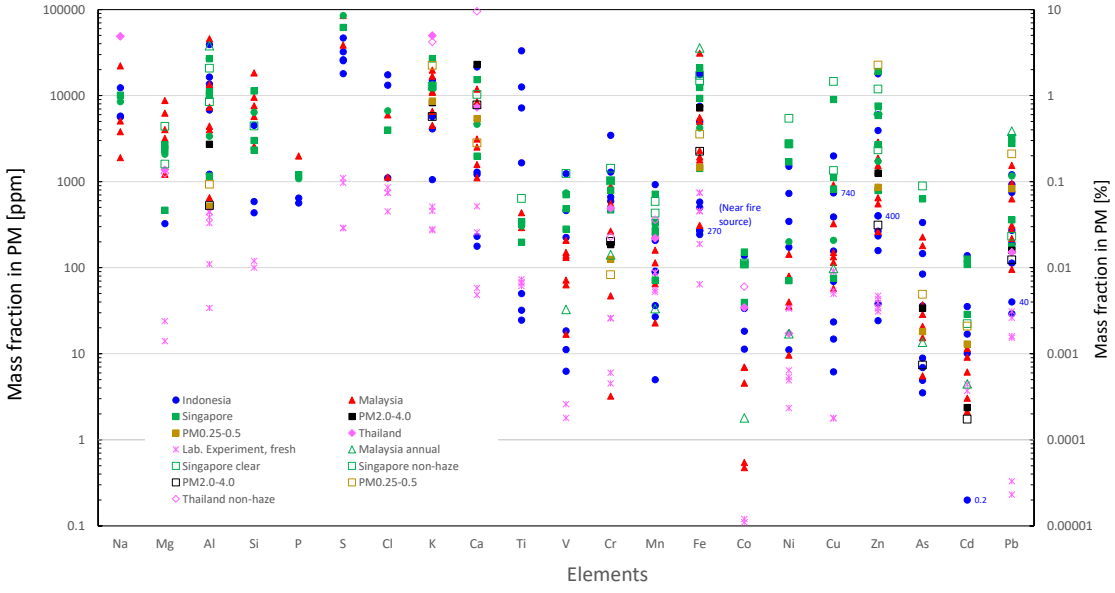

Fig. S4 Mass fractions of major elements in fine particles ($PM_{2.5\ or\ less}$) during haze and non-haze periods, and in laboratory-generated fresh smoke particles.

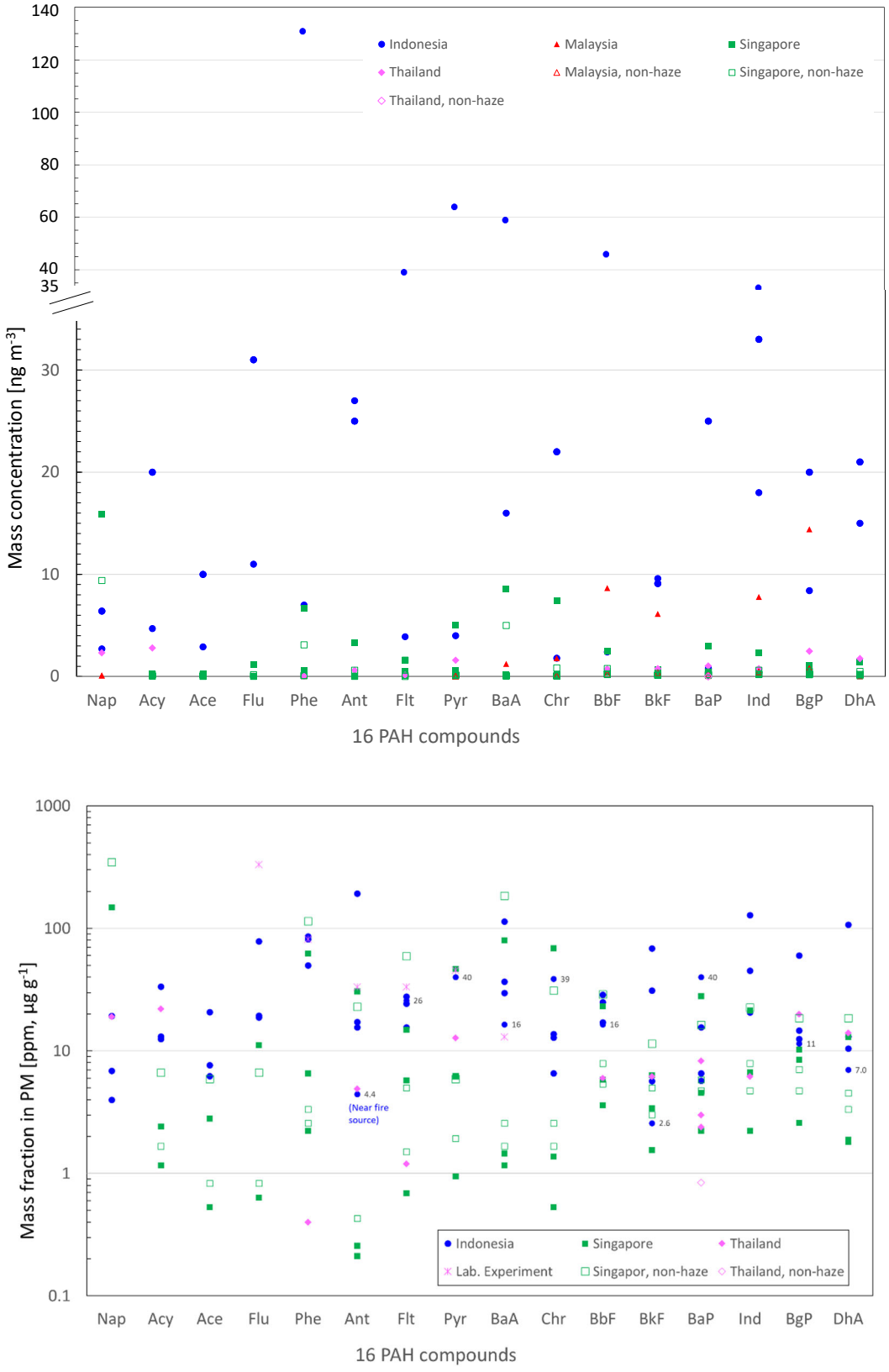

Fig. S5 Mass concentrations and mass fractions of 16 PAHs in PM (TSP, PM_{10} and $PM_{2.5}$) in PM during haze and non-haze periods. These data were obtained from the following studies: (upper) [24, 28, 37, 43, 51, 70, 72, 73, 82, 88, 119] and (lower) [26, 28, 37, 43, 72, 77, 92, 119].

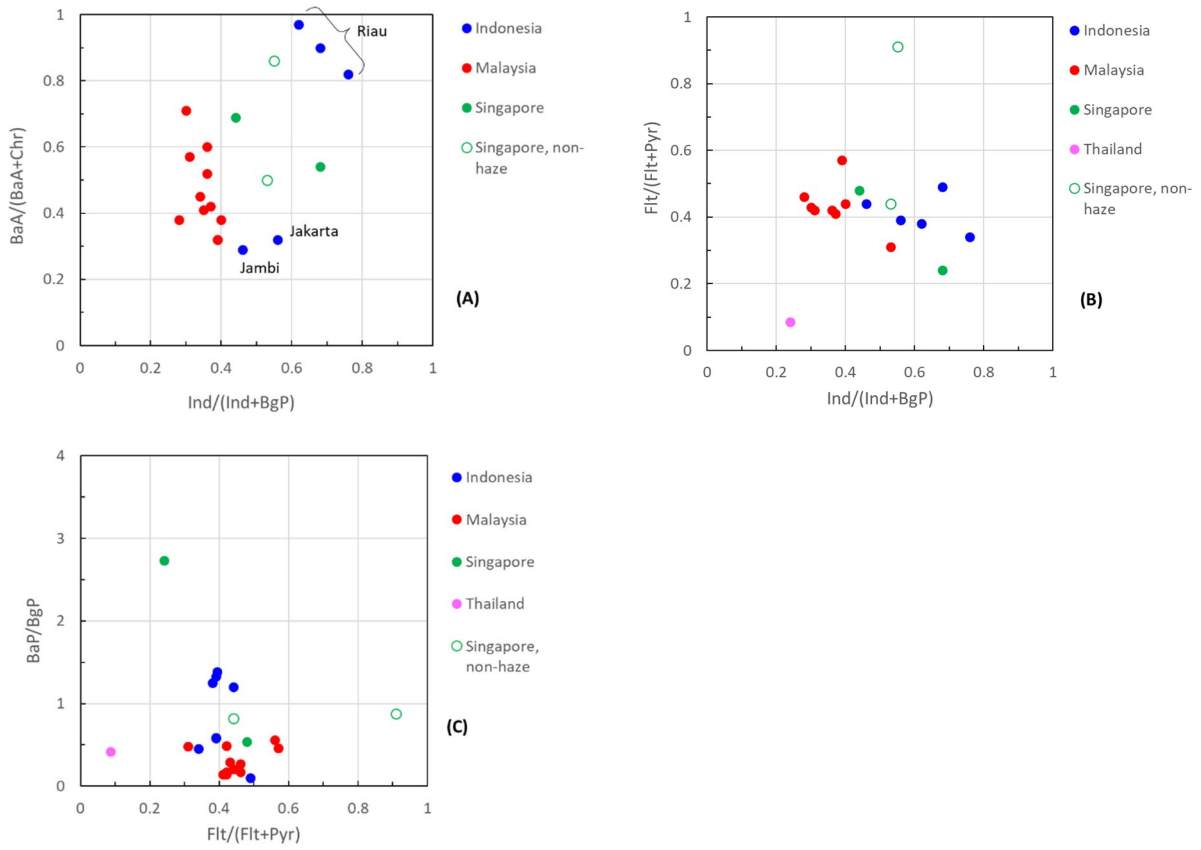

Fig. S6 PAH diagnostic ratios for PM. The data were obtained from the following studies: (A) [13, 24, 28, 37, 43, 51, 70, 108], (B) [13, 28, 37, 43, 51, 88, 92, 108], (C) [13, 28, 37, 43, 51, 77, 88, 92, 108].

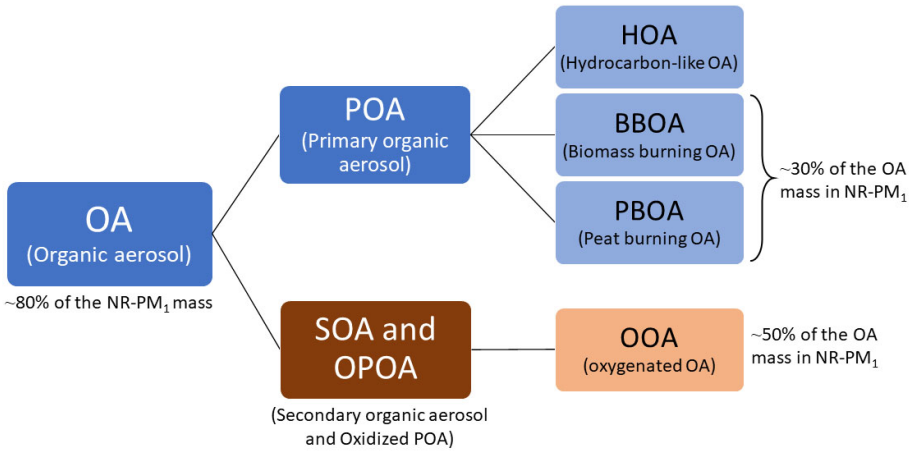

Fig. S7 Four source factors of OA identified in NR-PM_1 (haze particles) by ToF-ACSM.

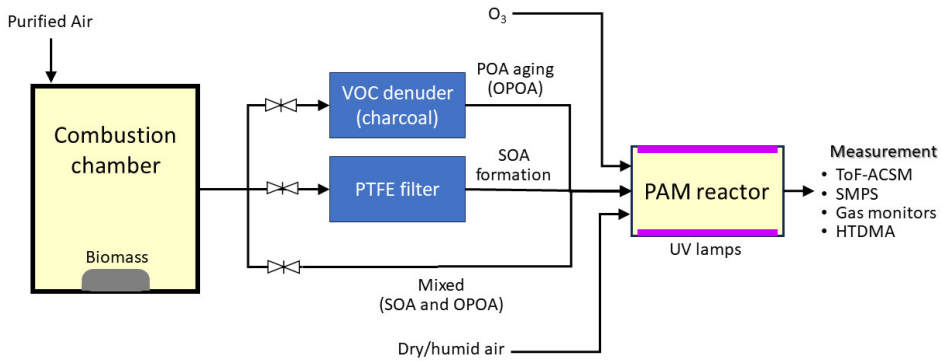

Fig. S8 Laboratory experimental system for separating POA aging (OPOA), SOA formation, and mixed POA aging and SOA formation[102, 109]. (Individual experiments performed by switching the corresponding valve.)